One-step synthesis of spherical α-$Ni(OH)_2$ nanoarchitectures

2006 Nanotechnology 17 4278

(http://iopscience.iop.org/0957-4484/17/16/046)

INSTITUTE OF PHYSICS PUBLISHING NANOTECHNOLOGY
Nanotechnology **17** (2006) 4278–4283 doi:10.1088/0957-4484/17/16/046

One-step synthesis of spherical α-$Ni(OH)_2$ nanoarchitectures

Yuanyuan Luo, Guanghai Li[1], Guotao Duan and Lide Zhang

Key Laboratory of Materials Physics, Anhui Key Laboratory of Nanomaterials and Nanotechnology, Institute of Solid State Physics, Chinese Academy of Sciences, Hefei 230031, People's Republic of China

E-mail: ghli@issp.ac.cn

Received 16 May 2006, in final form 27 June 2006
Published 7 August 2006
Online at stacks.iop.org/Nano/17/4278

Abstract

We report the synthesis of sphere-like α-$Ni(OH)_2$ nanoarchitecture by self-assembly with the aid of hexamethylenetetramine (HMT). The α-$Ni(OH)_2$ nanoarchitectures, with a diameter of several micrometres, are composed of many nanoflakelets about 10 nm in thickness. The influences of the reaction temperature, time, reagent, nickel salt and pH value on the morphology and structure of the α-$Ni(OH)_2$ were studied, the chemical and thermal stability are discussed, and the formation mechanism is proposed. The α-$Ni(OH)_2$ nanoarchitectures display a good electrochemical capacity.

(Some figures in this article are in colour only in the electronic version)

1. Introduction

Nickel hydroxide is a favourable cell material used as positive electrode in nickel-based rechargeable batteries [1–5]. $Ni(OH)_2$ exists in two polymorphic modifications, namely, α and β phases. The α-phase is isostructural with a hydrotalcite-like structure and contains stacked positively charged $Ni(OH)_{2-x}$ layers with exchangeable anions and water molecules intercalated into the interlayer space to balance the positive charges. The β-phase is structurally brucite-like and consists of an ordered stacking of well-oriented $Ni(OH)_2$ layers without any intercalated species. α-$Ni(OH)_2$ is a superior electrode material compared to its β-modification [6–8]. Although α-$Ni(OH)_2$ is less stable in strong alkaline media and with ageing than β-$Ni(OH)_2$, the use of additives in α-$Ni(OH)_2$ has been reported to make its layer structure stable and modify the electrochemical properties effectively [9, 10]. Thus, it is very meaningful to synthesize α-$Ni(OH)_2$ with high electrochemical capacity on a large scale.

Up to now, various $Ni(OH)_2$ nanoarchitectures have been prepared, including flowerlike [11], nanotubes [1], nanorods [12], mesoporous films [13], nanosheets [14–16], hollow spheres [17], nanoribbons [18], and stacks of pancakes [19]. To the best of our knowledge, only a few reports concern α-$Ni(OH)_2$ [11, 20–23]. Therefore, the fabrication of α-$Ni(OH)_2$ active materials with high surface area remains a considerable challenge.

In this paper, we report the one-step synthesis of α-$Ni(OH)_2$ sphere-like nanoarchitectures by a simple hydrothermal process with the aid of hexamethylenetetramine (HMT) in $NiCl_2$ aqueous solution. The electrochemical response shows that the α-$Ni(OH)_2$ electrode has a good electrochemical capacity.

2. Experimental details

In a typical preparation, 50 ml of 0.5 M aqueous solution of hexamethylenetetramine (HMT, $C_6H_{12}N_4$) were mixed with 25 ml of 1 M green aqueous solution of $NiCl_2{\cdot}6H_2O$ under constant stirring at room temperature in a closed flask until the solution became homogeneous and light green. The pH value of the solution was adjusted to about 6.5 by HCl. Then the mixture was kept in an oven at 90 °C for 6 h. Finally a large quantity of light green precipitates was filtered, washed several times with distilled water and ethanol, and finally dried at 75 °C. Some of the sample was mixed with 6 M KOH aqueous solution and kept in a closed flask in an oven at 90 °C for 3 h, and then washed and dried again. Some samples were heat-treated at 150 °C for 2 h inside an alumina boat in air with a heating rate of 2 °C min^{-1}.

X-ray diffraction (XRD) was performed on a Philips X'Pert diffractometer using the Cu Kα line. Infrared

[1] Author to whom any correspondence should be addressed.

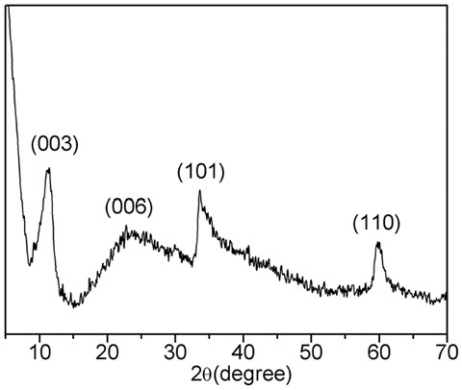

Figure 1. XRD pattern of nickel hydroxide prepared at 90 °C for 6 h.

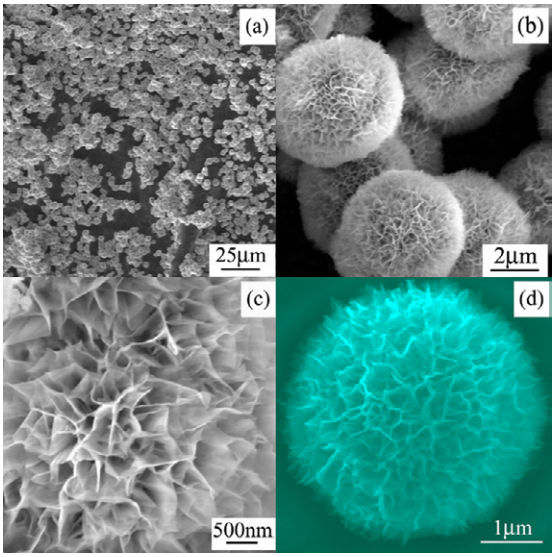

Figure 2. FESEM images of the α-Ni(OH)$_2$ spheres at different magnifications.

spectra were obtained by using a Fourier infrared spectrum instrument (Nicolet Magna-IR750) operating in transmission mode. The morphology was observed with a field emission scanning electron microscope (FE-SEM) (Sirion 200 FEG), a transmission electron microscope (TEM, JEM-2010) and high-resolution transmission electron microscope (HRTEM, JEOL 2010).

A nickel hydroxide electrode was prepared by filling a nickel form with a paste containing nickel hydroxide. The electrode was dried for 1 h at 80 °C. The electrochemical response was measured with a CHI660a analyser with an interpersonal computer in an electrochemical cell, which contains the nickel hydroxide working electrode, a Pt counter electrode, an Hg/HgO reference electrode, and 6 M KOH solution as the electrolyte. All tests were performed at room temperature.

3. Results and discussion

Figure 1 shows the XRD pattern of the products prepared at 90 °C for 6 h (sample A) on a glass substrate. All the diffraction peaks can be indexed as a hexagonal Ni(OH)$_2$ structure (α-Ni(OH)$_2$) [21, 24]. Due to the overlap of the (006) diffraction peak with the amorphous background from the glass substrate, it is hard to determine the exact position of the (006) reflection. Based on the (003) reflection one can determine the interlayer distance of α-Ni(OH)$_2$, and it is about 7.96 Å. In fact, as a hydrotalcite-like structure, the d values correspond to successive diffraction peaks from basal planes, i.e., $d_{(003)} \approx 2d_{(006)} \approx 3d_{(009)}$. Therefore, there is a (006) reflection in spite of the very weak intensity in figure 1, which is in good agreement with those reported previously [21, 22]. The existence of the (110) reflection shows a layer structure resulting from strongly divided hydroxyl layers and weak bonding interactions between intercalated ions and hydroxyl layers. In α-Ni(OH)$_2$ hexagonal structure, the c-axis is 23.88 Å according to the equation $c = 3d_{(003)}$, assuming a 3R polytypism for the hydrotalcite [25, 26], and the a-axis is 3.04 Å from $a = 2d_{(110)}$, corresponding to the result reported by Vicente Rives's group [27].

Figure 2 shows typical FE-SEM images of sample A. Many sphere-like α-Ni(OH)$_2$ nanostructures with a fairly uniform size of several micrometre in diameter can be seen. The local magnification image clearly shows the fine structure and building blocks of such spheres. The surface of the α-Ni(OH)$_2$ sphere is bestrewed with many nanoflakelets, forming a hierarchical network-like structure. Such nanoflakelets are of ultra-thinness (with a thickness less than 10 nm). They are easily distorted and tangled together.

TEM observations also display the layer structure of the α-Ni(OH)$_2$ spheres and give more information about the interior structure of the spheres. From figure 3 one can see that the nanosheets appear far into the interior of the spheres, and are of good transparency to the electron beam, indicating that the nanosheet is very thin. The nanosheets are very flexible and they can be bent at random and connected to each other. It is hard to obtain a single nanosheet due to its layer structure in spite of ultrasonication for sufficient time, and thus a ring-like ED pattern was obtained (see figure 3(b)), which comes from several nanosheets. The HRTEM observation at the tip of a nanosheet clearly shown that the lattice fringes are parallel to the surface of the nanosheet (see figure 3(c)), and it was found that the interplanar distance is about 7.9 Å, corresponding to the {003} crystal planes of α-Ni(OH)$_2$, which is in agreement with the XRD results.

To study the formation mechanism of the spherical α-Ni(OH)$_2$ nanoarchitectures, some of the products were taken out at different reaction times. After reaction at 90 °C for 30 min, a Ni(OH)$_2$ gel was formed (see figure 4(a)). The Ni(OH)$_2$ crystallites began to grow and assemble to form sphere-shaped structures as the reaction continued (see figure 4(b)), and finally individual spheres broke away from the gel; see figure 4(c).

To better understand the growth mechanism of the α-Ni(OH)$_2$ spheres, a series of experiments with different conditions were carried out. When the reaction temperature decreased from 90 to 75 °C, the average number of the nanoflakelets composing the Ni(OH)$_2$ spheres and the diameter of the Ni(OH)$_2$ sphere decreased noticeably; see figure 5(a). When the reaction was carried out at 120 °C in Teflon-lined autoclaves for 3 h, the average diameter of the sphere

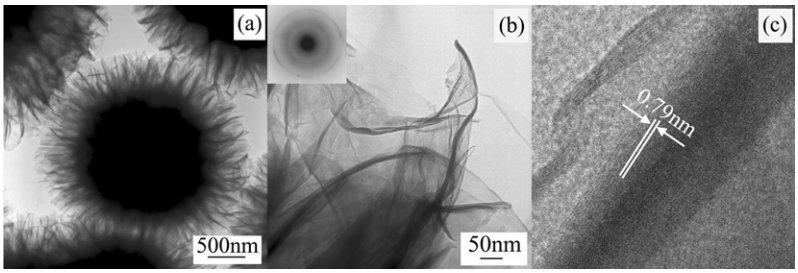

Figure 3. TEM images of the α-Ni(OH)$_2$ spheres: (a) individual spheres, (b) nanoflakelets and corresponding SAED, and (c) HRTEM image.

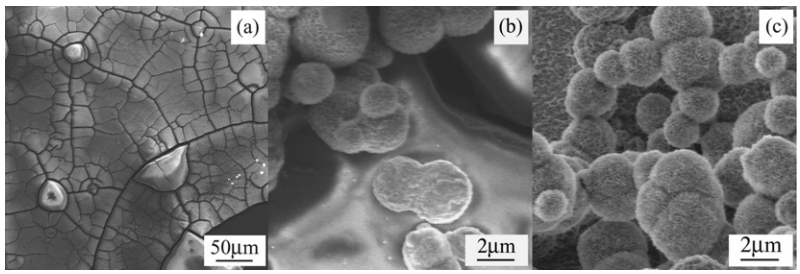

Figure 4. FESEM images of the α-Ni(OH)$_2$ spheres prepared at 90 °C for different times. (a) 30 min, (b) 60 min, and (c) 120 min.

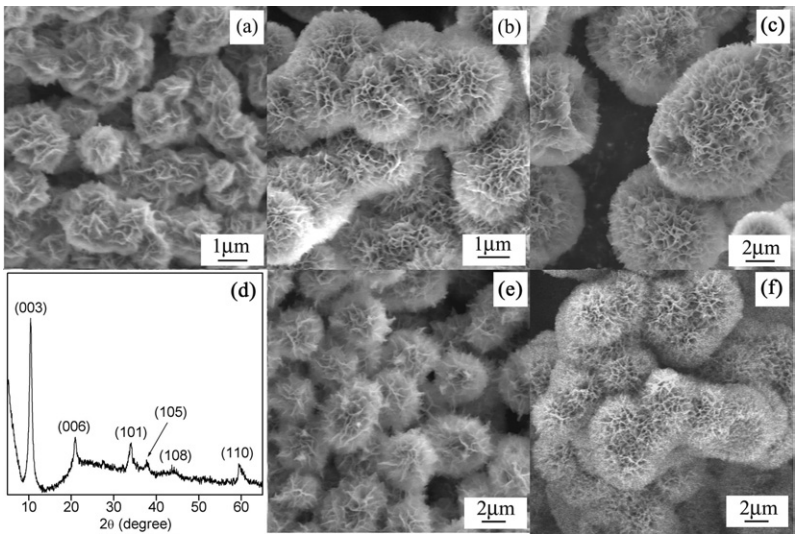

Figure 5. FESEM images of the α-Ni(OH)$_2$ spheres with different hydrothermal reaction conditions: 0.5 M HMT and 1 M $NiCl_2$ (a) at 75 °C for 6 h, (b) at 120 °C for 3 h and (c) at 90 °C for 6 days; (d) is the corresponding XRD pattern of (c); (e) 0.0025 M HMT and 1 M $NiCl_2$ at 90 °C for 6 h, and (f) 1 M HMT and 1 M $NiCl_2$ at 90 °C for 6 h.

increased, and some of them were even connected with each other; see figure 5(b). When the reaction time increased from 6 h to 6 days, the size of the α-Ni(OH)$_2$ spheres increased substantially; some new layers of the nanoflakelets were formed on the surface of old spheres, see figure 5(c), and the first XRD peak moved from 11.1° to 10.35°, see figures 1 and 5(d), which indicated that the interlayer distance has increased because the content of HMT organic matter 'hydroxyl' Cl^- anions and water intercalated into α-Ni(OH)$_2$ changed, compared with sample A (the corresponding FT-IR and XPS patterns are not shown here), and the layer structure of α-Ni(OH)$_2$ might be modulated [28, 29]. The appearance of the sharp diffraction peaks at 37.7° and 44.3° indicates the better crystallization of the α-Ni(OH)$_2$ with long reaction time. The above results show that the reaction temperature and the reaction time can affect the size and the crystallization phase of the spheres. High reaction temperature or long reaction time can promote the further growth of the spheres. When the content of the HMT was reduced to 5%, the α-Ni(OH)$_2$ spheres were underdeveloped and the number of the nanoflakelets forming the sphere decreased noticeably; see figure 5(e). But when the concentration of the HMT was doubled, the reaction took place faster and the time to form the α-Ni(OH)$_2$ spheres became shorter; see figure 5(f). Other reagents, such as ammonia, CTAB and urea, were also used instead of HMT, and it was found that no α-Ni(OH)$_2$ spheres

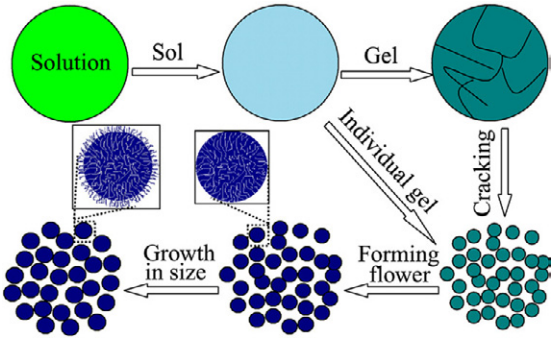

Figure 6. Schematic illustration of the formation mechanism of the α-Ni(OH)$_2$ spheres.

were formed at high temperature for a long reaction time with the same concentration solution. Thus, the HMT plays an important role in the formation of the α-Ni(OH)$_2$ spheres. It was also found that the α-Ni(OH)$_2$ spheres can be formed by using other nickel salts as the Ni^{2+} source, such as $Ni(NO_3)_2$, $NiSO_4$, $Ni(CH_3COO)_2$, indicating that the anion is not the main factor affecting the formation of α-Ni(OH)$_2$ spheres. Further experiments show that other solvents, such as alcohol and glycol, can only form Ni-based nanocrystallites (the XRD patterns are not shown here). It was found that the pH value of the solution affects the formation of α-Ni(OH)$_2$, and at a low pH (<4), there is no precipitate and at a high pH (>9) only β-Ni(OH)$_2$ was formed; thus the optimal choice of pH value is very important.

The above results indicate that the α-Ni(OH)$_2$ spheres are mainly formed from the Ni(OH)$_2$ gel. In the initial stage of hydrothermal treatment, some of the solved HMT might re-congregate and form small clusters with Ni(OH)$_2$ gel, which might react as nucleation centres of the Ni(OH)$_2$ spheres; some of the Ni(OH)$_2$ sol might transform to large gel with the aid of the HMT, and the gel may break down and form a large number of sphere-like cells, which also act as the nucleation centres of the α-Ni(OH)$_2$ spheres. With the increase in reaction time or reaction temperature, the α-Ni(OH)$_2$ spheres grow further. The formation of an α-Ni(OH)$_2$ sphere undergoes different phases, such as the formation of sol and gel, breaking down from the gel, self-assembly and enlargement of α-Ni(OH)$_2$ spheres, as schematically indicated in figure 6. α-Ni(OH)$_2$ is a layered compound of the CdI_2 type, and the nature of its 2D layer structures leads to the anisotropy of the bonding power. A weak bonding power exists between the layers, while a strong bonding power is in the layer-plane, and this imbalance is enhanced with the increase of the interlayer distance. A larger interlayer distance will weaken the binding power between layers, leading to the rupture along the *c*-axis more easily, and thus resulting in the formation of the α-Ni(OH)$_2$ nanoflakelets [17]. Our experiments demonstrate that the synthesis of high specific surface area α-Ni(OH)$_2$ spherical nanoarchitecture is very easy with the aid of HMT reagent.

The formation process of the α-Ni(OH)$_2$ spheres in present study is different from that reported in the literature. Zeng's group reported the synthesis of hollow ZnO dandelions with single-crystalline building units by a modified Kirkendall process [30] and CuO microspheres by a two-tiered organizing scheme [31], while Han's group reported the formation of a three-dimensional dendritic nanostructure of copper hydroxide through a progressive process [32]. In the present study, the formation of sphere-like α-Ni(OH)$_2$ is a one-step self-assembly process, in which the HMT reacts as the nucleation centre or helps to form the Ni(OH)$_2$ gel.

Table 1. Reduction potential E_R, oxidation potential E_O, $E_O - E_R$ for α-Ni(OH)$_2$ and β-Ni(OH)$_2$ electrodes at room temperature.

	Potentials (mV)		
Electrode	E_R	E_O	$E_O - E_R$
α-Ni(OH)$_2$	168	245	77
β-Ni(OH)$_2$	160	245	85

The stability of the as-synthesized α-Ni(OH)$_2$ in strong alkaline solution was further studied. After treatment with 6 M KOH solution at 90 °C for 3 h, it was found that the Ni(OH)$_2$ is still in the α-phase, and the interlayer distance decreases due to ions exchanging, i.e., HMT organic matter and Cl^- anions will be replaced by the hydroxyl ions or more water molecules will intercalate into the α-Ni(OH)$_2$ interlayer, and this leads to the reorientation of the layer structure of the α-Ni(OH)$_2$ [28, 29]. No phase transformation of the α-Ni(OH)$_2$ spheres was found after heat treating at 150 °C for 2 h. The corresponding SEM images after treatment with 6 M KOH solution and heat-treating at 150 °C all indicate that the spherical structure still exists. This result indicates that the α-Ni(OH)$_2$ spheres synthesized in this study have a relatively high chemical stability and thermal stability as compared with other α-Ni(OH)$_2$ materials [33]. It is believed that the stability of the as-synthesized α-Ni(OH)$_2$ in the strong alkaline solution and by ageing is closely related to the intercalated ions. Such α-Ni(OH)$_2$ material not only has higher surface-to-volume ratio and sphere-like structure but also has good basic and thermal stability. They are expected to be used as good cell active materials [34].

Figure 7 shows the electrochemical response of the spherical α-Ni(OH)$_2$ nanoarchitectures. For comparison, pure β-Ni(OH)$_2$ powders were also examined. The corresponding parameters of two kinds of positive electrode are summarized in table 1. From the voltammogram curves (figure 7(a)), one can see that the cathode and anode peak current densities of the α-Ni(OH)$_2$ spheres are higher than those of β-Ni(OH)$_2$ powders, which suggests that the α-Ni(OH)$_2$ spheres have a higher electrochemical reactivity and a faster activation. The difference between the oxidation potential and the reduction potential is taken as $E_O - E_R$. The value of $E_O - E_R$ for the α-Ni(OH)$_2$ spheres electrodes is lower than that for β-Ni(OH)$_2$ powder electrodes. Figure 7(b) shows the galvanostatic charge–discharge results of α-Ni(OH)$_2$ spheres and β-Ni(OH)$_2$ powders in 6 M KOH electrolyte. The charge curve of the β-Ni(OH)$_2$ is steep and the charge potential increases quickly with the charging. The oxygen reaction of the β-Ni(OH)$_2$ powders appears earlier than the α-Ni(OH)$_2$ spheres. The specific discharge capacities are about 280.5 and 211.0 mA h g^{-1} for the α-Ni(OH)$_2$ spheres and pure β-Ni(OH)$_2$ powders, respectively. From this primary result one can deduce that there are obvious

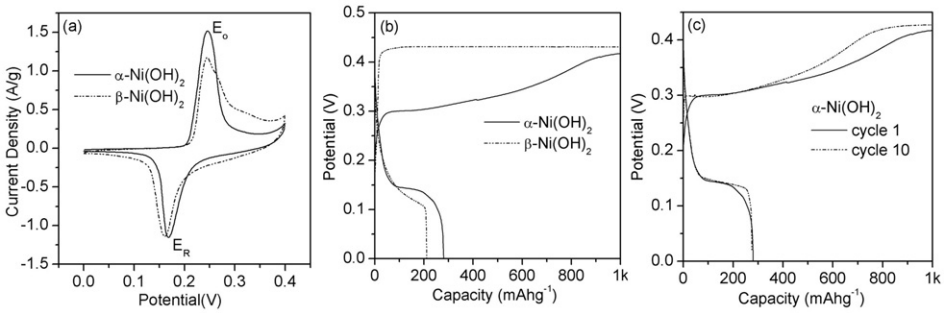

Figure 7. (a) Cyclic voltammograms, scan rate: 20 mV s^{-1} (versus HgO/Hg 6 M KOH), (b) charge–discharge curves at 150 mA g^{-1} of spherical α-Ni(OH)$_2$ nanoarchitectures and pure β-Ni(OH)$_2$ powders and (c) charge–discharge curves at 150 mA g^{-1} of spherical α-Ni(OH)$_2$ nanoarchitectures at the first and tenth cycles.

advantages for the spherical α-Ni(OH)$_2$ nanoarchitectures, i.e. higher discharge potential and longer plateau, indicating that the α-Ni(OH)$_2$ electrodes display better electrochemical capacity than the β-Ni(OH)$_2$ electrodes. Figure 7(c) shows the charge–discharge curves of α-Ni(OH)$_2$ spheres in 6 M KOH electrolyte at the first and tenth cycle. The α-Ni(OH)$_2$ almost remains constant in capacity and discharge potential from cycle 1 to 10, indicating that the α-Ni(OH)$_2$ spheres have a stable electrochemical response. The sphere-like α-Ni(OH)$_2$ consists of many nanosheets, which are radially and closely stacked with each other to form a three-dimensional network. The spheres are also full of pores between nanosheets, and this pore structure can shorten the proton diffusion distance and increase its velocity, and thus lower the local polarization. Nevertheless, as is well known, in the discharge/charge processes, α-Ni(OH)$_2$ will convert to β-Ni(OH)$_2$ with time, and thus lower the electrochemical capacity [9, 10]. In the present study, the stability of α-Ni(OH)$_2$ has been substantially improved as compared with other α-Ni(OH)$_2$ materials [33]. However, FTIR analysis shows evidence that some α-Ni(OH)$_2$ has converted to β-Ni(OH)$_2$ after more than ten discharge/charge processes, which is disadvantageous to their applications. Further work should be addressed to improve the stability of α-Ni(OH)$_2$ spheres by special modification or adding some additives, which will bring about wide application and large commercial efficiency.

4. Conclusion

In conclusion, spherical α-Ni(OH)$_2$ nanoarchitectures were synthesized by a one-step self-assembly process. The spheres, with a size of several micrometres, are composed of nanoflakelets of about 10 nm in thickness. It was found the HMT plays a critical role in the formation of the nanoarchitecture, in which the HMT not only provides OH^-, but also helps to form the Ni(OH)$_2$ gel, which reacts as the nucleation centres of the spheres, and no spheres are formed when other reagents are used. The water reagent is a very important factor in controlling the formation of α-Ni(OH)$_2$ spheres, and other solvents, such as alcohol and glycol, can only form Ni(OH)$_2$ nanocrystallites. The pH value is also an important factor in controlling the formation of the α-Ni(OH)$_2$. At a low pH (<4), there is no precipitate and at a high pH (>9), only β-Ni(OH)$_2$ was formed. Such high specific surface area α-Ni(OH)$_2$ nanoarchitectures possess a relatively high chemical and thermal stability upon treating with 6 M KOH solution or heat-treating at 150 °C. Electrochemical responses show that the α-Ni(OH)$_2$ electrode has a good electrochemical capacity, and it may be expected to be used as positive-electrode material for rechargeable batteries.

Acknowledgments

We gratefully acknowledge the financial support of the National Basic Research Program of China under Grant No. G 2005CB623603. We also are grateful to Professor Mingtai Wang, Dr Changneng Zhang and Dr Li Guo, from the Institute of Plasma Physics, Chinese Academy of Sciences, for help in the electrochemical experiments.

References

[1] Cai F S, Zhang G Y, Chen J, Gou X L, Liu H K and Dou S X 2004 *Angew. Chem.* **116** 4308
[2] Nelson P A, Elliott J M, Attard G S and Owen J R 2002 *Chem. Mater.* **14** 524
[3] Hu W K and Noréus D 2003 *Chem. Mater.* **15** 974
[4] Watanabe K, Kikuoka T and Kumagai N 1995 *J. Appl. Electrochem.* **25** 219
[5] Hooper A and McGeehin P 1981 *Phys. Technol.* **12** 45
[6] Indria L, Dixit M and Kamath P V 1994 *J. Power Sources* **52** 93
[7] Barnard R, Randell C F and Tye F L 1980 *J. Appl. Electrochem.* **10** 109
[8] Faure C, Delmas C and Willmann P 1991 *J. Power Sources* **36** 497
[9] Zhu W H, Ke J J, Yu H M and Zhang D J 1995 *J. Power Sources* **56** 75
[10] Liu B, Yuan H T, Zhang Y S, Zhou Z X and Song D Y 1999 *J. Power Sources* **79** 277
[11] Liu B H, Yu S H, Chen S F and Wu C Y 2006 *J. Phys. Chem.* B **110** 4039
[12] Matsui K, Kyotani T and Tomita A 2002 *Adv. Mater.* **14** 1216
[13] Tan Y W, Srinivasan S and Choi K S 2005 *J. Am. Chem. Soc.* **127** 3596
[14] Liang Z H, Zhu Y J and Hu X L 2004 *J. Phys. Chem.* B **108** 3488
[15] Chen D L and Gao L 2005 *Chem. Phys. Lett.* **405** 159
[16] Liu X H, Qiu G Z, Wang Z and Li X G 2005 *Nanotechnology* **16** 1400
[17] Wang D B, Song C X, Hu Z S and Fu X 2005 *J. Phys. Chem.* B **109** 1125

[18] Yang D N, Wang R M, Zhang J and Liu Z F 2004 *J. Phys. Chem.* B **108** 7531
[19] Coudun C and Hochepied J F 2005 *J. Phys. Chem.* B **109** 6069
[20] Jayashree R S and Kamath P V 1999 *J. Appl. Electrochem.* **29** 449
[21] Jeevanandam P, Koltypin Y and Gedanken A 2001 *Nano Lett.* **1** 263
[22] Soler-Illia G J de A A, Jobbágy M, Regazzoni A E and Blesa M A 1999 *Chem. Mater.* **11** 3140
[23] Akinc M, Jongen N, Lemaître J and Hofmann H 1998 *J. Eur. Ceram. Soc.* **18** 1559
[24] Freitas M B J G 2001 *J. Power Sources* **93** 163
[25] Uzunova E, Klissurski D and Kassabov S 1994 *J. Mater. Chem.* **4** 153
[26] Bookin A S, Cherkashin V I and Drits A 1993 *Clays. Clay. Mineral.* **41** 558
[27] Labajos F M, Sastre M D, Trujillano R and Rives V 1999 *J. Mater. Chem.* **9** 1033
[28] Radha A V, Vishnu Kamath P and Shivakumara C 2005 *Solid State Sci.* **7** 1180
[29] Wang Z, Lan T and Pinnavaia T J 1996 *Chem. Mater.* **8** 2200
[30] Liu B and Zeng H C 2004 *J. Am. Chem. Soc.* **126** 16744
[31] Liu B and Zeng H C 2004 *J. Am. Chem. Soc.* **126** 8124
[32] Zhang Z P, Shao X Q, Yu H D, Wang Y B and Han M Y 2005 *Chem. Mater.* **17** 332
[33] Bode H, Dehmelt K and Witte J 1966 *Electrochim. Acta* **11** 1079
[34] Yuan Y F, Tu J P, Wu H M, Li Y and Shi D Q 2005 *Nanotechnology* **16** 803